Carcinogenesis vol.35 no.1 pp.123–130, 2014
doi:10.1093/carcin/bgt266
Advance Access publication August 12, 2013

The P110 subunit of PI3-K is a therapeutic target of acacetin in skin cancer

Sung Keun Jung[1–3,†], Jong Eun Kim[1,2,4,†], Sung-Young Lee[1], Mee Hyun Lee[1], Sanguine Byun[1,2,4], Young A.Kim[2], Tae Gyu Lim[1,2,4], Kanamata Reddy[1], Zunnan Huang[1], Ann M.Bode[1], Hyong Joo Lee[2,4], Ki Won Lee[1,2,4,*] and Zigang Dong[1]

[1]The Hormel Institute, University of Minnesota, 801 16th Ave NE, Austin, MN 55912, USA, [2]WCU Biomodulation Major, Department of Agricultural Biotechnology, Seoul National University, Seoul 151-921, Republic of Korea, [3]Division of metabolism and Functionality Research, Korea Food Research Institute, Seongnam 463-746, Republic of Korea and [4]Advanced Institutes of Convergence Technology, Seoul National University, Suwon, 443-270, Republic of Korea

*To whom correspondence should be addressed. Tel: +82 2 880 4661;
Fax: +82 2 878 6178;
Email: kiwon@snu.ac.kr
Correspondence may also be addressed to Zigang Dong. Tel: +1 507 437 9600;
Fax: +1 507 437 9606;
Email: zgdong@hi.umn.edu

The identification of primary molecular targets of cancer-preventive phytochemicals is essential for a comprehensive understanding of their mechanism of action. In the present study, we investigated the chemopreventive effects and molecular targets of acacetin, a flavonoid found in *Robinia pseudoacacia*, also known as black locust. Acacetin treatment significantly suppressed epidermal growth factor (EGF)-induced cell transformation. Immunoblot analysis revealed that acacetin attenuated EGF-induced phosphorylation of Akt and p70^{S6K}, which are downstream effectors of phosphatidylinositol 3-kinase (PI3-K). An immunoprecipitation kinase assay of PI3-K and pull-down assay results demonstrated that acacetin substantially inhibits PI3-K activity by direct physical binding. Acacetin exhibited stronger inhibitory effects against anchorage-dependent and -independent cell growth in cells expressing higher PI3-K activity compared with those exhibiting relatively low PI3-K activity. Binding assay data combined with computational modeling suggest that acacetin binds in an adenosine triphosphate (ATP)-competitive manner with the p110α subunit of PI3-K and interacts with Val828, Glu826, Asp911, Trp760, Ile777, Ile825, Tyr813, Ile910 and Met900 residues. Acacetin was also found to significantly reduce SK-MEL-28 tumor growth and Akt phosphorylation *in vivo*. Taken together, these results indicate that acacetin is an ATP-competitive PI3-K inhibitor and a promising agent for melanoma chemoprevention.

Introduction

Skin cancer is the most frequently diagnosed cancer in the world and the three most common forms are melanoma, squamous cell carcinoma and basal cell carcinoma (1). Melanoma is considered as one of the most aggressive human cancers and is frequently resistant to therapy (2). The phosphatidylinositol 3-kinase (PI3-K) pathway is often deregulated in melanoma, and its activation leads to the phosphorylation of Akt (also known as protein kinase B). Akt is a potent oncoprotein that influences numerous downstream factors, promoting cell survival and proliferation. In melanoma, the Akt phosphorylation status has been suggested to inversely correspond with patient survival (3). Therefore, the inhibition of PI3-K represents an attractive strategy for melanoma treatment and prevention.

Abbreviations: ATP, adenosine triphosphate; EGF, epidermal growth factor; ERK, extracellular signal-regulated kinase; FBS, fetal bovine serum; KD, kinase dead; MEM, minimum essential medium; PI3-K, phosphatidylinositol 3-kinase.

PI3-K is a heterodimeric signaling factor composed of a p85 regulatory subunit and a p110α catalytic subunit, which upon activation is responsible for the conversion of phosphatidylinositol-4,5-bisphosphate to phosphatidylinositol-2,4,5-trisphosphate. This leads to the recruitment and phosphorylation of Akt, and the promotion of cell growth and proliferation (4). Hyperactivity or overexpression of PI3-K has been observed in skin carcinogenesis and melanoma (5,6). We recently demonstrated that ultraviolet irradiation, a potent inducer of skin cancer, activates Akt and its downstream substrate p70^{S6K} in a mouse model of skin carcinogenesis (7).

Acacetin (5,7-dihydroxy-4′-methoxyflavone, Figure 1) is a flavonoid present in *Robinia pseudoacacia*, also known as black locust, and has been shown to have antioxidant, anti-inflammatory and anticancer effects (8,9). Acacetin has also been shown to inhibit lipopolysaccharide-induced cyclooxygenase-2 and inducible nitric oxide synthase expression by suppressing PI3-K/Akt/Ikk and mitogen-activated protein kinase signaling pathways (8). Recent studies showed that acacetin regulates mitogen-activated protein kinases signaling including MLK3/MKK3/6 and p38 (9,10). However, the direct molecular target and mechanisms of action for acacetin in suppressing skin cancer remain to be fully investigated.

Here, we report that acacetin is an adenosine triphosphate (ATP)-competitive inhibitor of PI3-K and suppresses epidermal growth factor (EGF)-induced cell transformation and melanoma cell growth. This resulted in the downregulation of Akt phosphorylation in SK-MEL-28 xenograft tumors in nude mice. These findings shed further light into the mechanisms of action behind acacetin's potent chemopreventive properties in melanoma.

Materials and methods

Materials

Acacetin (95%) and EGF were purchased from Sigma–Aldrich (St Louis, MO). LY294002 was obtained from Calbiochem (Darmstadt, Germany). Eagle's minimum essential medium (MEM), gentamicin and L-glutamine were obtained from Gibco BRL (Carlsbad, CA). Fetal bovine serum (FBS) was purchased from Gemini Bio-Products (Calabasas, CA). Antibodies against phosphorylated p90RSK (Thr359/Ser363), phosphorylated Akt (Ser 473), total Akt, phosphorylated p70^{S6K}, total p70^{S6K} and total p90^{RSK} were purchased from Cell Signaling Technology (Beverly, MA). Antibodies against phosphorylated extracellular signal-regulated kinase 1/2 (ERK1/2) (Thr202/Tyr204), total ERKs and the PI3-Kp110α subunit were obtained from Santa Cruz Biotechnology (Santa Cruz, CA). The antibody against β-actin was obtained from Sigma–Aldrich and the active PI3-K protein was obtained from EMD Millipore (Billerica, MA). ATP and the chemiluminescence detection kit were purchased from GE Healthcare Biosciences (Pittsburgh, PA) and the protein assay kit was obtained from Bio-Rad Laboratories (Hercules, CA).

Cell culture and transfections

JB6 P$^+$ mouse skin epidermal cells (5% FBS–MEM), SK-MEL-5 and SK-MEL-28 (10% FBS–MEM) were cultured at 37°C and 5% CO_2 in growth medium supplemented with antibiotics. Cells were maintained by subculturing

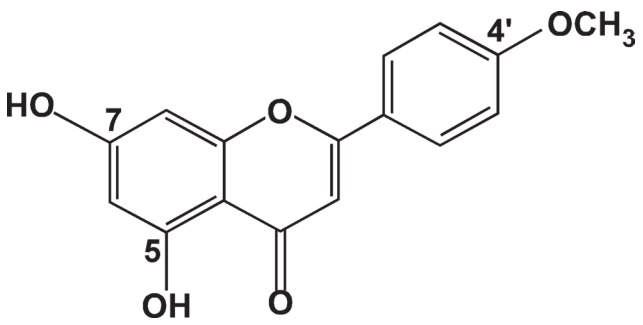

Fig. 1. The chemical structure of acacetin.

†These authors contributed equally to this work.

at 80–90% confluence and media were changed every 3 days. For transfection experiments, cells were split and the expression vector was transfected using jetPEI (Polyplus-transfection, Illkirch, France), following the manufacturer's suggested protocol when cells reached 50–60% confluence. For stable transfection, JB6 P^+ cells (5.0×10^5) in 5% FBS–MEM were seeded in 100 mm culture dishes. After culturing at 37°C in 5% CO_2 for 16 h, the cells were transfected using jetPEI with 2 μg of constitutively active, wild-type p110α, kinase dead (KD)-p110α or pcDNA3.1 (mock) vector. Stably transfected cells were obtained through selection for G418 resistance (400 μg/ml) and further confirmed through the assessment of PI3-K activity and expression.

Anchorage-independent cell transformation assay

Tumor cells were suspended in Basal Medium Eagle medium and added to 0.6% agar, with the indicated concentrations of acacetin in the base layer and a top layer of 0.3% agar. For the JB6 P^+ line, cells were further exposed to EGF (10 ng/ml) during treatment with acacetin or vehicle control. The cultures were maintained at 37°C in a 5% CO_2 incubator for 1–2 weeks and then colonies were counted under a microscope using Image-Pro Plus software (V.4) (Media Cybernetics, Silver Spring, MD).

Cell viability

Cells were seeded (1×10^3 cells per well) in 96-well plates, incubated for 24 h and then treated with the indicated doses of each compound. After incubation for 1, 2 or 3 days, 20 μl of CellTiter 96 AQueous One Solution (Promega, Medison, WI) were added and cells were incubated for 1 h at 37°C in a 5% CO_2 incubator. Absorbance was measured at 492 nm.

Western blot assays

Cells (1.5×10^6) were cultured in 100 mm dishes for 48 h, and then serum starved in 0.1% FBS–MEM for 24 h. The cells were then treated with acacetin (0, 5, 10 and 20 μM) for 1 h before exposure to 10 ng/ml EGF for an additional 30 min. Cells were harvested and disrupted with lysis buffer before protein concentration was measured using a dye-binding protein assay kit (Bio-Rad Laboratories) as described in the manufacturer's manual. Protein lysates (40 μg) were subjected to 10% sodium dodecyl sulfate–polyacrylamide gel electrophoresis and transferred to polyvinylidene difluoride membranes (EMD Millipore). After transfer, the membranes were incubated with the specific primary antibodies at 4°C overnight. Protein bands were visualized by a chemiluminescence detection kit after hybridization with a horseradish peroxidase-conjugated secondary antibody.

PI3-K assay

Cultured cells were disrupted with lysis buffer and 500 μg of protein lysate were mixed with protein-conjugated A/G beads (20 μl) for 1 h at 4°C. After centrifugation of the mixture, the supernatant fraction was mixed with the PI3-K antibody (2 μg) and gently rocked overnight at 4°C. These tubes were centrifuged and the beads were washed three times. The mixtures were then incubated with 20 μl (0.5 mg/ml) phosphatidylinositol (Avanti Polar Lipids) for 5 min at room temperature, followed by incubation with reaction buffer (100 mM HEPES, pH 7.6, 50 mM $MgCl_2$, 250 μM ATP containing 10 μCi of [γ-^{32}P]-ATP) for an additional 10 min at 30°C. The reaction was stopped by adding 15 μl of 4 N HCl and 130 μl of chloroform:methanol (1:1). After vortexing, 30 μl of the lower chloroform phase was spotted onto a 1% potassium oxalate-coated silica gel plate, which was previously activated for 1 h at 110°C. The resulting ^{32}P-labeled phosphatidylinositol-2,4,5-trisphosphate was separated by thin layer chromatography and radiolabeled spots were visualized by autoradiography.

In vitro *and* ex vivo *immunoprecipitation assay*

Active PI3-K (100 ng) or the cellular supernatant fraction of disrupted JB6 P^+ cells (500 μg) was incubated with either acacetin-conjugated Sepharose 4B beads or Sepharose 4B beads alone (100 μl, 50% slurry) in reaction buffer (11). After incubation with gentle rocking overnight at 4°C, the beads were washed five times with buffer, and the proteins bound to the beads were analyzed by immunoblotting.

Cell cycle analysis

Cells (7×10^4) were seeded in a 60 mm dish and cultured for 24 h before treatment for 48 h with the indicated concentrations of acacetin. The cells were harvested by trypsinization, fixed with ethanol, stained with propidium iodide and then analyzed for cell cycle phase by flow cytometry.

Computational modeling

The three-dimensional structure of PI3-K was obtained from the SWISS-MODEL Repository (12) and the molecular geometry coordinates of acacetin were obtained from the PubChem compound database (http://pubchem.ncbi.nlm.nih.gov). Prior to ligand–protein docking calculations, the raw PDB structure was converted into an all-atom, fully prepared receptor model structure by using the Protein Preparation Wizard module, whereas the original two-dimensional structure of acacetin was converted to a three-dimensional model using LigPrep. Protein–ligand docking simulations were computed using the high-performance hierarchical docking algorithm Glide (13). The final structure of the PI3-K–acacetin binding model was generated using Schrödinger induced fit docking (14), which merges the predictive power of Prime with the docking and scoring capabilities of Glide for calculating the most likely protein conformational changes upon ligand binding.

Xenograft mouse model

The experimental protocols were approved by the Animal Care and Use Committee of Seoul National University. Athymic nude mice (5-week-old; mean body weight 20 g) were obtained from Orient (Seoul, Korea). Animals were acclimated to the facility for 1 week before the study began and had free access to food and water. Mice were divided into three groups: (i) vehicle only ($n = 10$); (ii) 1 mg/kg of acacetin ($n = 10$) and (iii) 5 mg/kg of acacetin ($n = 10$). SK-MEL-28 cells (1×10^7 cells/100 μl) were suspended in MEM and inoculated with 100 μl matrigel subcutaneously into the right flank of each mouse. Vehicle or acacetin was intraperitoneally injected three times per week for 1 month. Tumor volume was calculated using measurements of two diameters of the individual tumor base using the formula: tumor volume (mm^3) = (length × width × height × 0.5). Mice were monitored until tumors reached 1 cm^3 in total volume and were euthanized for further studies. All procedures were conducted in accordance with the accepted Seoul National University guidelines for the use and care of laboratory animals.

Immunohistochemistry

For an immunohistochemical analysis of Akt phosphorylation, excised tumors were fixed in 10% formalin for 1 day, embedded in paraffin and cut into 5 μm thick sections. Serial sections were mounted on Silane-coated slides, deparaffinized three times with xylene and dehydrated through a gradient alcohol series. The deparaffinized sections were boiled in 0.01 mol/l citrate buffer (pH 6.0) for 15 min for antigen retrieval. Sections were washed in phosphate-buffered saline with Tween 20 and placed in blocking buffer for 30 min, followed by incubation with a primary antibody against pAkt (Ser 473; Cell Signaling Technology, 1:50 dilution) for 12 h at 4°C. Next, the endogenous peroxidase activity of paraffin-embedded sections was treated with 3% hydrogen peroxide for 10 min in blocking solution, consisting of phosphate-buffered saline with 1% bovine serum albumin. The slides were then incubated with anti-rabbit horseradish peroxidase-conjugated secondary antibody for 30 min. The immunoreactive complexes were detected by staining with 3,3′-diaminobenzidine tetrahydrochloride hydrate and counterstained with Mayer's hematoxylin. All slides were scored by two observers. The staining intensity and pattern were evaluated using a 0 to 3+ scale (0, completely negative; 1+, weak; 2+, intermediate; 3+, strong). A final score of ≥2+ or greater was required for the case to be considered positive.

Statistical analysis

As necessary, data are expressed as means ± standard error of the mean or SD and significant differences were determined using one-way analysis of variance. Duncan's multiple range test was used to determine the means that were significantly different. A probability value of $P < 0.05$ was used as the criterion for statistical significance.

Results

Acacetin inhibits EGF-induced cell transformation

The EGF-induced cell transformation assay is designed for the analysis of chemopreventive effects of natural phytochemicals (15,16). We first determined whether acacetin could affect EGF-induced neoplastic cell transformation. Acacetin (Figure 1) was found to significantly inhibit EGF-induced cell transformation in JB6 P^+ cells without affecting cell viability (Figure 2A–C). Next, to determine the influence of acacetin on cellular signaling during EGF-induced cell transformation, we analyzed the effects of treatment on ERKs and Akt activation. Acacetin completely suppressed EGF-induced Akt and $p70^{S6K}$ phosphorylation without affecting ERKs signaling (Figure 2D). Because PI3-K is the most prominent upstream kinase of Akt, we hypothesized that acacetin might be directly binding to and inhibiting PI3-K activity. Acacetin was found to strongly suppress EGF-induced PI3-K activity in JB6 P^+ cells (Figure 2E). Furthermore, a pull-down assay using acacetin-conjugated Sepharose beads showed that acacetin physically binds with the PI3-K protein (Figure 2F). Taken together, these results indicate that the inhibition of EGF-induced Akt phosphorylation by

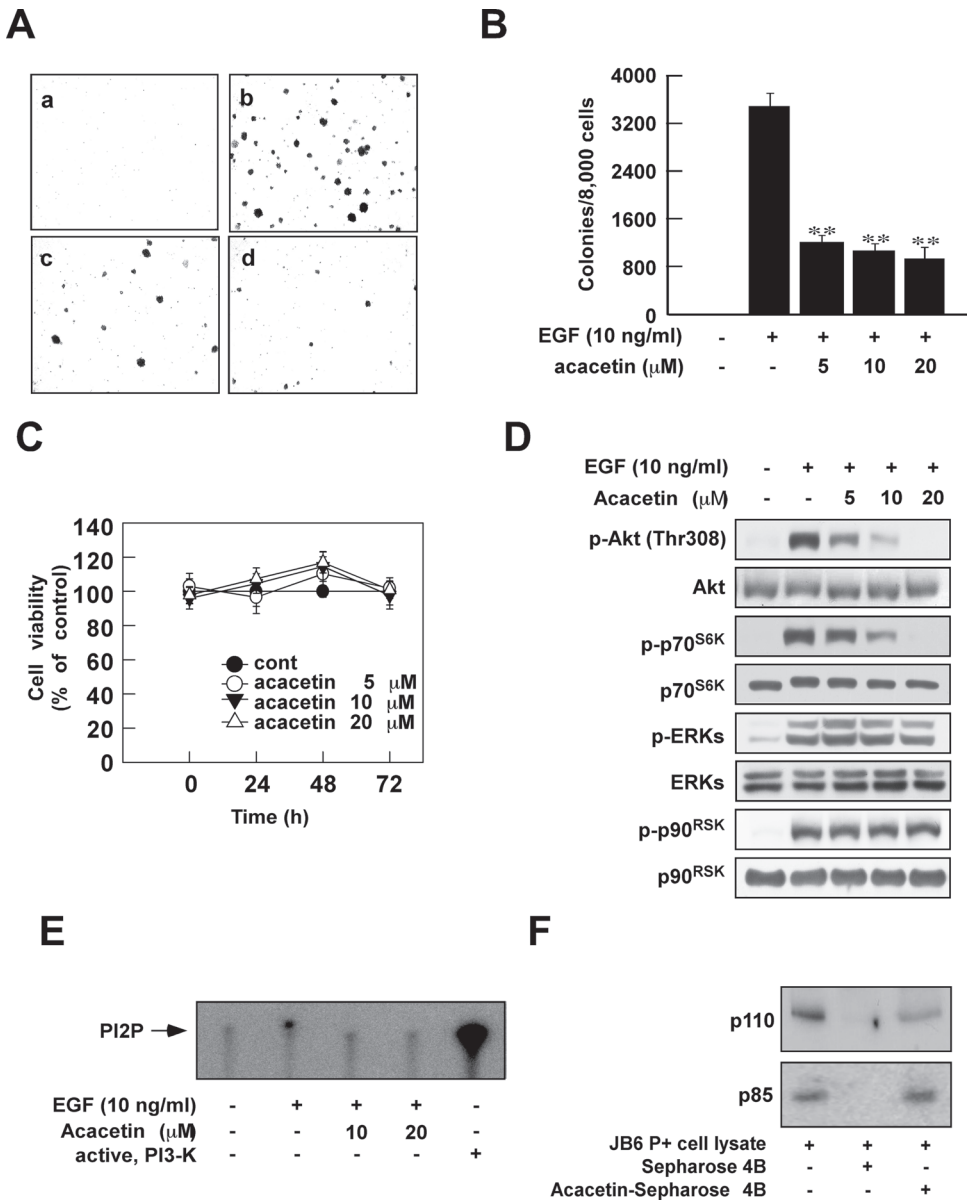

Fig. 2. Acacetin inhibits EGF-induced anchorage-independent cell growth by targeting PI3-K. (**A** and **B**) Acacetin inhibits EGF-induced JB6 cell transformation. JB6 cells were treated as described in Materials and methods and colonies were counted 14 days later: untreated control (a); EGF (10 ng/ml) alone (b); EGF and 10 μM acacetin (c); EGF and 20 μM acacetin (d). Data are shown as means ± SD of the colony numbers as determined from three separate experiments. The asterisk indicates significant differences between groups treated with EGF and acacetin together and the group treated with EGF alone (**$P < 0.01$). (**C**) Acacetin does not affect cell viability in JB6 cell. Cell viability was measured as described in Materials and methods. (**D**) Acacetin inhibits EGF-induced phosphorylation of Akt (Ser308) and p70S6K in JB6 cells. Western blot analysis was performed as described in Materials and methods using the indicated antibody. (**E** and **F**) Acacetin directly inhibits EGF-induced PI3-K activity by binding with PI3-K in JB6 cells. Kinase (**E**) and acacetin pull-down assays (**F**) were performed as described in Materials and methods.

acacetin is due to the direct binding of acacetin to PI3-K and subsequent inhibition of its activity.

PI3-K plays a key role in EGF-induced anchorage-independent cell growth and is directly inhibited by acacetin

Using constitutively active- and mock-plasmid-transfected JB6 P^+ cells, our objective was to examine the role of PI3-K in EGF-induced anchorage-independent cell growth. Constitutively active-p110α-transfected JB6 cells grew faster and generated more colonies than mock-transfected JB6 P^+ cells (Figure 3A and B). Transfection of KD-p110α inhibited phosphorylation of Akt (Figure 3C), retarded the growth of JB6 P^+ cells (Figure 3E) and inhibited EGF-induced anchorage-independent cell growth (Figure 3E). We next compared the effect of acacetin treatment on EGF-induced anchorage-independent growth of wild-type and KD-p110α-transfected JB6 P^+ cells. KD-p110α-transfected JB6 P^+ cells exhibited significantly reduced sensitivity toward acacetin treatment compared with those transfected with wild-type p110α (Figure 3F).

SK-MEL-28 cells are more sensitive than SK-MEL-5 cells to the inhibitory effect of acacetin on anchorage-dependent and -independent growth

We hypothesized that cells exhibiting higher levels of PI3-K activity would be more sensitive to acacetin treatment due to its suppression of PI3-K activity. Among the eight cell lines tested, we selected the SK-MEL-28 cell line (which exhibits relatively higher Akt phosphorylation) and the SK-MEL-5 cell line (which exhibits relatively lower Akt phosphorylation) for further study (Figure 4Aa). PI3-K

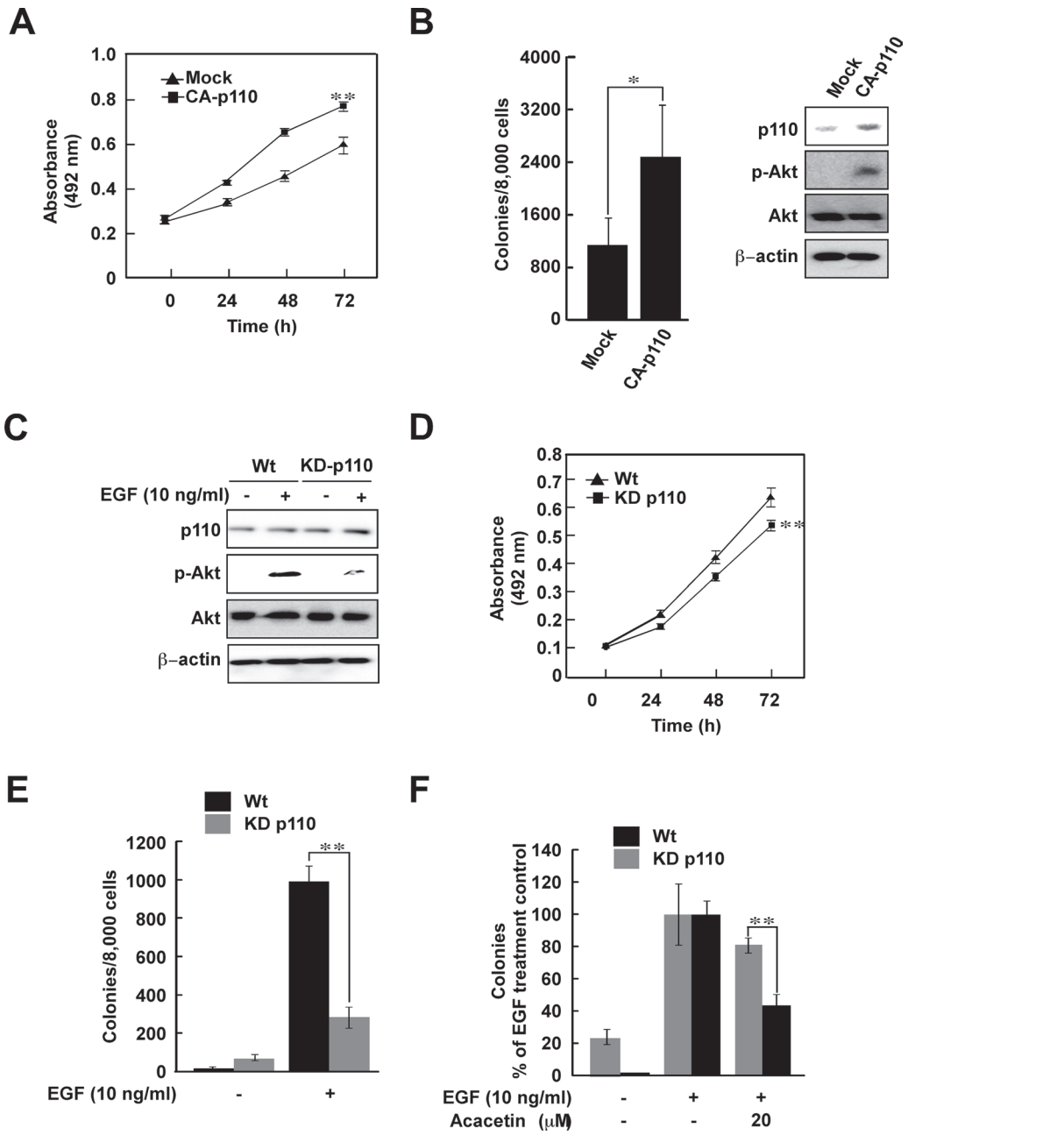

Fig. 3. PI3-K plays a critical role in EGF-induced anchorage-independent cell growth and the inhibitory effect of acacetin is PI3-K-dependent. (**A** and **B**) Anchorage-dependent (**A**) and -independent (**B**) growth of constitutively active (CA)-p110-transfected JB6 cells is faster than that of mock-transfected JB6 cells. Cell proliferation and anchorage-independent cell growth was examined as described in Materials and methods. Efficiency of transfection was measured by western blot (right panel). Data are shown as means ± SD of colony numbers as determined from three separate experiments. The asterisks (* or **) indicate significant ($P < 0.05$ or $P < 0.01$, respectively) differences between CA-p110- and mock-transfected JB6 groups. (**C**–**E**) Transfection of a KD-p110 plasmid inhibits growth of JB6 cells. Efficiency of transfection was measured by western blot (**C**). Cell proliferation was measured by MTS (3-(4,5-dimethylthiazol-2-yl)-5-(3-carboxymethoxyphenyl)-2-(4-sulfophenyl)-2H-tetrazolium) assay (**D**). Transfection of KD-p110 inhibits EGF-induced anchorage-independent cell growth (**E**). Anchorage-independent cell growth was determined as described in Materials and methods. The asterisks indicate significant differences between wild-type (Wt) and KD-p110-transfected JB6 groups (*$P < 0.05$ and **$P < 0.01$). (**F**) Inhibitory effects of acacetin on EGF-induced anchorage-independent cell growth are dependent on PI3-K activity. Stably transfected Wt and KD-p110 JB6 cells were treated with acacetin and anchorage-independent cell growth was measured as described in Materials and methods. Data are shown as means ± SD of colony numbers as determined from three separate experiments. The asterisk(s) indicates a significant difference between groups treated with acacetin and the untreated control group (*$P < 0.05$ and **$P < 0.01$).

immunoprecipitation analysis and kinase assay results demonstrated that SK-MEL-28 cells exhibited higher PI3-K activity compared with the activity in SK-MEL-5 cells (Figure 4Ab). The SK-MEL-28 cell line exhibited faster anchorage-dependent and -independent growth compared with SK-MEL-5 cells (Figure 4B). Next, we compared the effect of acacetin and the PI3-K inhibitor LY294002 on anchorage-dependent and -independent cell growth. Both acacetin and LY294002 exhibited a greater inhibitory effect against anchorage-dependent and -independent growth of SK-MEL-28 cells compared with SK-MEL-5 cells (Figure 4C and D). In SK-MEL-28 cells, acacetin also inhibited the phosphorylation of Akt and GSK3β, which are downstream effectors of PI3-K (Figure 4E). PI3-K inhibition has been shown to induce G_0/G_1 cell cycle arrest (17), and we also observed this effect as a result of acacetin treatment (Figure 4F). These results support our prior findings that PI3-K is a physical target of acacetin.

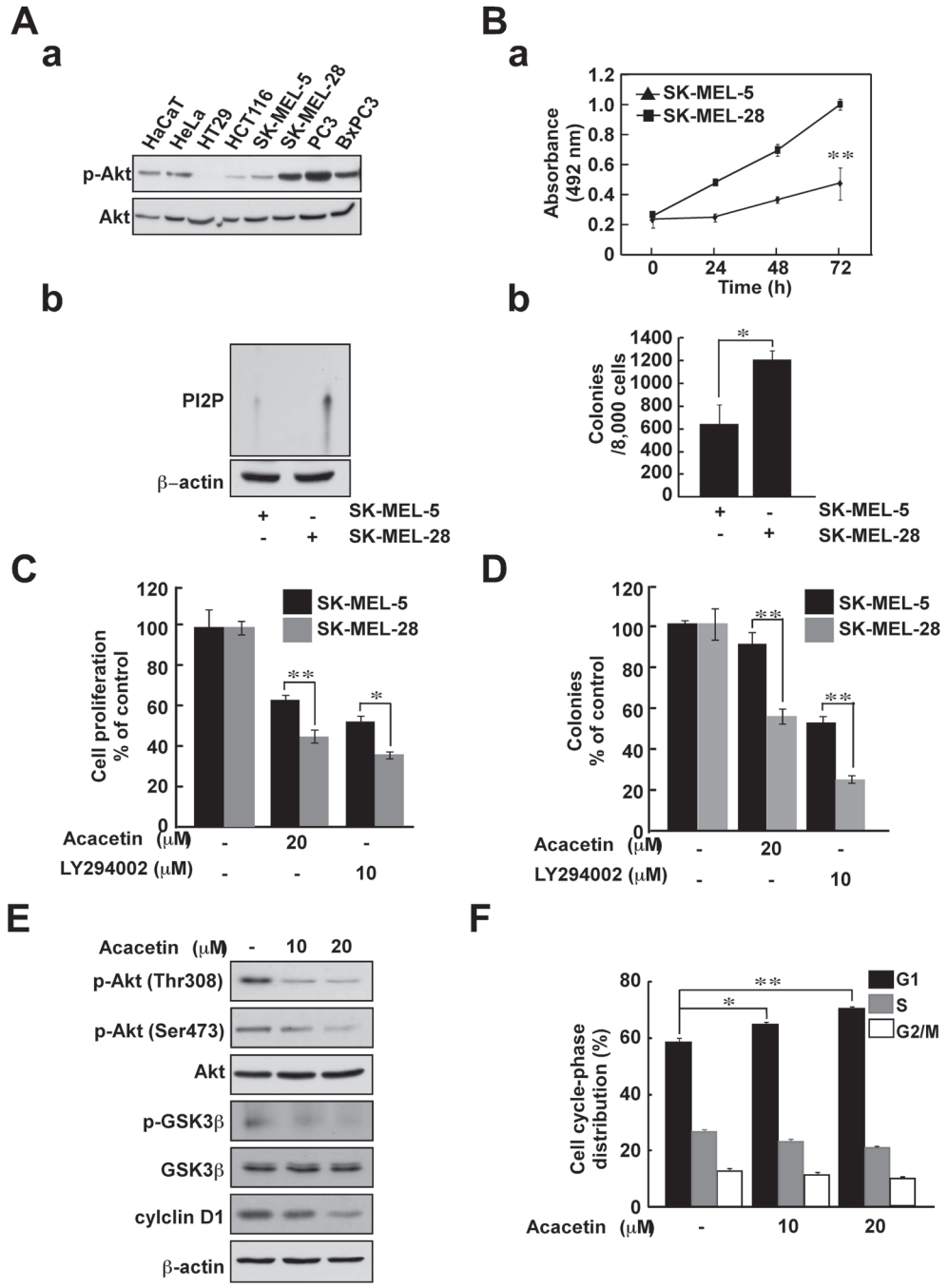

Fig. 4. SK-MEL-28 cells are more sensitive to the inhibitory effect of acacetin against anchorage-dependent and -independent cell growth compared with SK-MEL-5 cells. (**A**) Screening for cell lines that show higher PI3-K activity. Akt phosphorylation was investigated by western blot (a). SK-MEL-28 cells have higher PI3-K activity compared with SK-MEL-5 cells. PI3-K activity was measured after immunoprecipitation with a PI3-K antibody (b). (**B**) SK-MEL-28 anchorage-dependent (a) and -independent (b) cell growth is faster than that of SK-MEL-5 cells. Anchorage-dependent cell growth was measured using the MTS assay. Anchorage-independent cell growth was measured by soft agar assay. Anchorage-dependent and -independent cell growth was examined as described as Materials and methods. The asterisk indicates significant differences between the SK-MEL-5 and SK-MEL-28 cell groups (**$P < 0.01$). (**C** and **D**) Acacetin inhibits anchorage-dependent (**C**) and -independent (**D**) SK-MEL-28 cell growth more strongly than that of SK-MEL-5 cells. SK-MEL-28 and SK-MEL-5 cells were treated with acacetin and LY294002 (20 μM). (**E**) Acacetin inhibits PI3-K downstream signaling. SK-MEL-28 cells were treated with acacetin for 24 h in medium containing 10% FBS and then analyzed by western blot. (**F**) Cell cycle analysis of SK-MEL-5 and SK-MEL-28 cells treated with acacetin. Cells were not treated or treated with acacetin (0–20 μM) for 48 h. Cell cycle analysis was performed by flow cytometry. Data are shown as means ± SD. The asterisk indicates a significant difference between groups treated with acacetin and the untreated control group (*$P < 0.05$ and **$P < 0.01$).

Acacetin inhibits PI3-K activity in an ATP-competitive manner

Immunoprecipitation assay results demonstrated that acacetin directly binds with PI3-K in an ATP-competitive manner (Figure 5A and B). We therefore hypothesized that acacetin might dock with PI3-K in the ATP-binding pocket. To further investigate this idea, we performed an *in silico* docking study using the induced fit docking module. The hierarchical docking algorithm Glide of Schrödinger-Maestro v9.2 was then used to assess the possible binding orientations of PI3-K and acacetin (13). The simulation returned a positive result, with the theoretical acacetin–PI3-K complex as shown in Figure 5C and D.

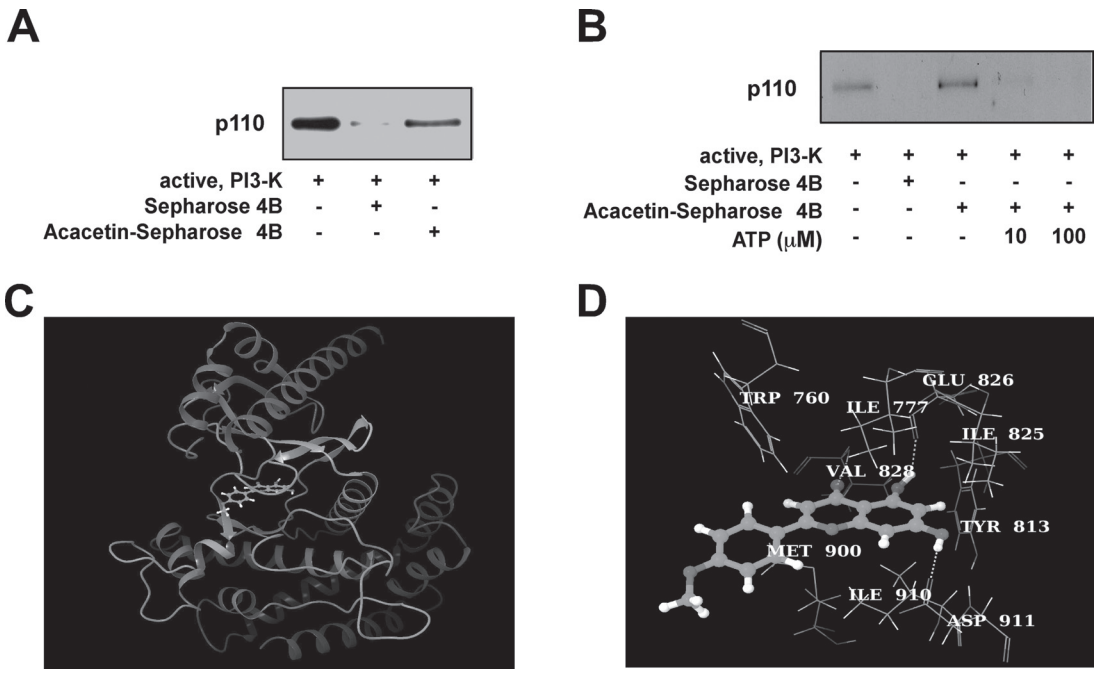

Fig. 5. Acacetin directly binds to PI3-K. (**A**) Acacetin directly binds with PI3-K. The direct binding of PI3-K and acacetin was confirmed by immunoblotting with a PI3-K antibody. Lane 1 (input control), PI3-K protein standard; lane 2 (control), Sepharose 4B beads alone cannot pull down PI3-K, as described in Materials and methods; lane 3, PI3-K pulled down using acacetin–Sepharose 4B affinity beads. (**B**) Acacetin binds with PI3-K in an ATP-competitive manner. Active PI3-K (100 ng) was incubated with ATP at different concentrations (0, 10 or 100 μM) and 100 μl of acacetin–Sepharose 4B or 100 μl of Sepharose 4B (as a negative control) in reaction buffer at a final volume of 500 μl. The mixtures were incubated at 4°C overnight with shaking. After washing, the pulled down proteins were detected by western blotting: lane 2, negative control, PI3-K cannot bind with Sepharose 4B; lane 3, positive control, PI3-K binding with acacetin–Sepharose 4B; lanes 4 and 5, increasing amounts of ATP decreased the binding of acacetin with PI3-K. Each experiment was performed three times. (**C** and **D**) Predicted models of the PI3-K–acacetin complex. The α-helices are drawn as cylinders and the β-strands as arrows. Acacetin is shown in stick model and protein residues are shown in line model. The figures were generated using VMD and Maestro. (**C**) The binding pose of acacetin inside the ATP-binding site of PI3-K. Here, only the kinase domain (sequence between Ser675 and Trp1027) of PI3-K delta is shown for clarity. (**D**) The interaction between acacetin and several residues in the ATP-binding pocket. Acacetin formed hydrogen bonds with Val828, Glu826 and Asp911. In addition, the protein residues, Trp760, Ile777, Ile825, Tyr813, Ile910 and Met900 showed hydrophobic interactions with the acacetin aromatic rings.

Acacetin suppresses SK-MEL-28 xenograft growth and Akt phosphorylation in tumors from nude mice

We used an *in vivo* xenograft model to further confirm the antitumorigenic activity of acacetin. Body weight loss or dramatic changes in appearance were not observed in mice treated with acacetin, indicating that the doses used were not overtly toxic to the animals (data not shown). As expected, acacetin treatment suppressed melanoma tumor development in mice (Figure 6A). The average volume of tumors in untreated mice increased over time, reaching a volume of 550 mm^3 at 4 weeks postinoculation. However, in mice treated with 1 or 5 mg/kg acacetin, the average tumor volume was 331 or 198 mm^3, respectively (Figure 6B). To further confirm the inhibitory effects of acacetin *in vivo*, we examined the level of Akt phosphorylation using immunohistochemical analysis of the extracted tumors. Consistent with our *in vitro* findings, the levels of Akt phosphorylation in the acacetin-treated groups were significantly reduced compared with the untreated controls (Figure 6C and D). Collectively, these results show that acacetin suppresses the tumorigenicity of SK-MEL-28 cells *in vivo*.

Discussion

Evidence from epidemiological studies shows that higher consumption of fruits and vegetables is linked to a lower risk of various cancers (18–20). Recent studies have shown that a number of phytochemicals can influence cancer-associated cell signaling pathways through the direct inhibition of specific enzymes (21). The physical inhibition of such enzymes is a more likely explanation for the strong bioactivity of various phytochemicals at low concentrations. Therefore, identifying the direct targets of phytochemicals is crucial for understanding the wider implications of treatment on alternative signaling pathways and provides a clearer perspective on the mechanism of action. We therefore placed a priority on identifying the physical molecular target of acacetin, while verifying its inhibitory effect on downstream effectors and treatment outcomes as a result of binding.

Malignant cell transformation is a process by which normal cells acquire the properties of cancer, giving rise to carcinogenesis. Exposure to carcinogens such as EGF and 12-*O*-tetradecanoylphorbol-13-acetate induces such transformation (16). EGF is a growth factor, which plays an important role in the regulation of cell proliferation, growth and differentiation (22). JB6 P^+ (promotion-sensitive) cells and tumor promoter-induced cell transformation comprise an optimal system to investigate the chemopreventive effects of phytochemicals (23). We have previously reported that EGF can induce cell transformation by activating multiple signaling pathways in JB6 P^+ cells (15,16). Evidence from several studies suggests that compounds capable of blocking EGF-induced cell transformation might be effective candidates for chemoprevention of skin cancer (16,24,25). One of weakness in this experimental model is the difficulty in translating to an appropriate animal experiment. We believe that the best animal model in which to confirm our results is the xenograft model using SK-MEL-28 cells, which express a high level of PI3-K activity. Therefore, we examined the chemopreventive effect of acacetin in the JB6 P^+ mouse skin model and the anticancer effects *in vitro* and *in vivo* in this study.

Melanoma remains the most lethal form of skin cancer (26). In many cases, tumors do not respond well to conventional chemotherapy. Since the discovery of the BRAF mutation as a critical driving factor in melanoma development, significant advances have been made (27). Small molecule inhibitors targeting the BRAF/mitogen-activated protein kinase pathway have been proposed as new treatment modalities

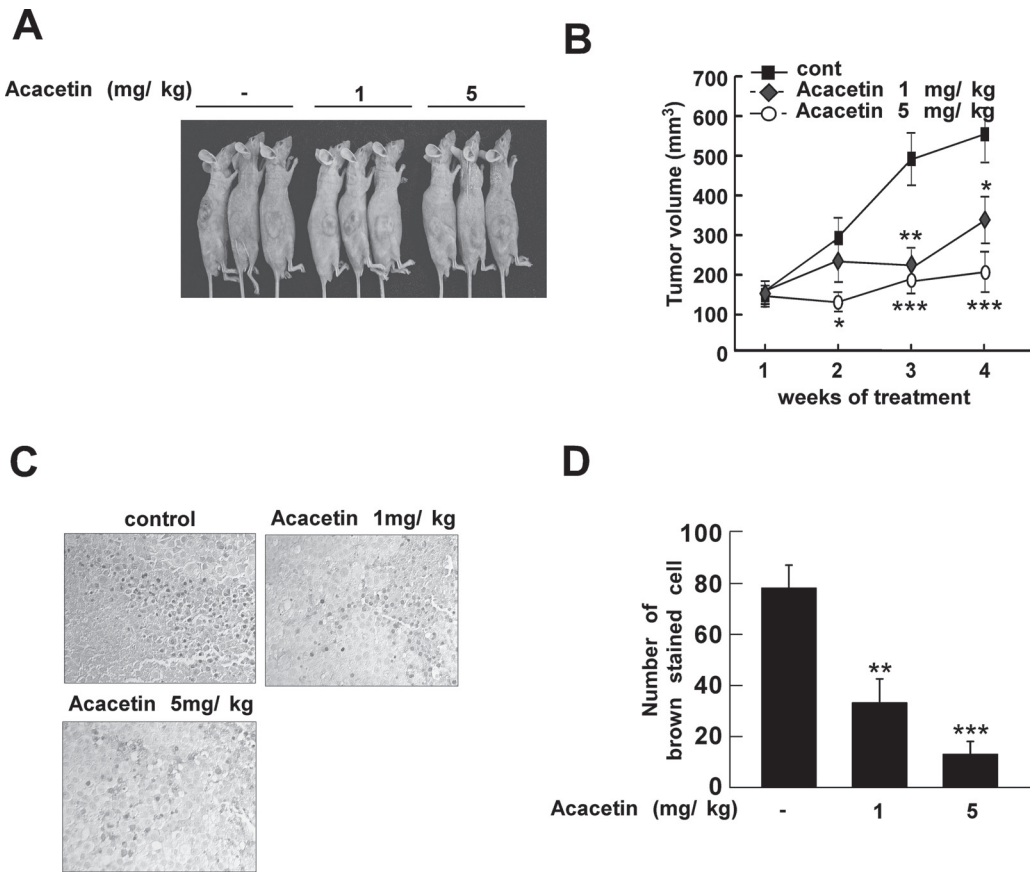

Fig. 6. Acacetin inhibits tumor growth and Akt phosphorylation in an SK-MEL-28 xenograft mouse model. (**A**) Photographs of mice from each group. (**B**) The average tumor volume of control and acacetin-treated mice plotted over 28 days after tumor cell inoculation. (**C** and **D**) Acacetin inhibits Akt phosphorylation in xenograft tumors grown in athymic nude mice. The immunostaining data are representative of three tissue samples from each group and Akt phosphorylation appears in brown. Phospho-Akt positive cells are counted as described in Materials and methods. Data are shown as means ± SD of six tumors. The *P* values indicate statistical significance of the inhibition of tumor growth by acacetin (*$P < 0.05$, **$P < 0.01$, ***$P < 0.001$).

(28). BRAF inhibitors such as PLX4032 and PLX4720 have shown initial positive responses against melanoma. However, the majority of cases are later hampered by the development of drug resistance (26). Another major signaling pathway important in melanoma development is the PI3-K/Akt pathway. The activation of this signaling cascade leads to increased chemoresistance and cancer cell survival (29). Therefore, targeting the PI3-K/Akt pathway with small molecule inhibitors could help overcome drug resistance toward BRAF inhibitors (30). In line with this idea, suppression of the PI3-K/Akt pathway has been reported to sensitize previously resistant melanoma cells tocisplatin and temozolomide (31).

In this study, we found that acacetin directly suppressed EGF-induced PI3-K activity and Akt/p70S6K signaling and subsequently inhibited EGF-induced anchorage-independent cell growth in JB6 P^+ cells. Our previous studies suggested that PI3-K is a promising target of phytochemicals to prevent cancer development because of its critical role in carcinogenesis and metastasis *in vitro* and *in vivo* (32,33). In addition, we compared the effects of acacetin on cell lines with differential PI3-K expression to better understand acacetin's mechanism of action. Because acacetin demonstrated a stronger inhibitory effect against cells expressing higher PI3-K activity, we identified PI3-K as a likely molecular target. Acacetin also showed stronger inhibitory effects against anchorage-dependent and -independent growth of melanoma cells with higher PI3-K expression. Suppression of PI3-K activity by transfection with KD-p110α reduced the effect of acacetin on EGF-induced anchorage-independent cell growth. We therefore concluded that PI3-K was likely to be a major target of acacetin in the suppression of anchorage-dependent and -independent melanoma growth. Acacetin might also have additional cellular targets that could also influence the apoptotic capacity of malignant cells, and this warrants further investigation.

Our PI3-K activity assay and immunoprecipitation results demonstrate that acacetin significantly inhibits PI3-K activity, and this effect occurs through direct physical binding. We additionally discovered that this interaction occurs in an ATP-competitive manner. A previous study showed that flavonoids such as myricetin and quercetin bind to PI3-K similar to the pharmaceutical inhibitors, wortmannin or LY294002, as shown by the X-ray crystallographic structures of PI3-K (34). To further aid in our understanding of the physical dimensions of this process, we used *in silico* analysis to generate a computational model of the acacetin/PI3-K complex (Figure 5). The binding orientation of acacetin and PI3-K obtained from induced fit docking data suggested that acacetin could locate within two regions of the ATP-binding pocket (Figure 5C and D), the 'adenine' pocket and hydrophobic region II, located at the mouth of the active site. The possibility exists that acacetin forms three hydrogen bonds with PI3-K: two involved with the backbone of the hinge residues Val828 and Glu826, and the other formed with the side chain (carboxylate oxygen) of Asp911 (Figure 5D). In addition, several residues in the PI3-K ATP-binding pocket, including Trp760, Ile777, Ile825, Tyr813, Ile910 and Met900 were estimated to participate in further hydrophobic interactions with the aromatic rings of acacetin. These results add a new perspective to our understanding of the parameters involved in PI3-K inhibition by acacetin. Further studies using X-ray crystallography or nuclear magnetic resonance techniques are needed to confirm the exact binding mode of acacetin to PI3-K.

The compound LY294002 is widely used in studies requiring PI3-K inhibition. However, this compound has not been developed for

therapeutic application due to the existence of non-specific targets (35). The PI3-K protein family represents a class of kinases that are structurally similar but appear to influence diverse downstream processes (35). Therefore, agents that can inhibit a specific isoform without targeting other family members are needed. The investigation of natural phytochemicals for anticancer activity by inhibiting PI3-K holds a number of advantages over approaches involving synthetic compounds. The generation of synthetic analogs is time consuming and requires careful verification of proper synthesis. In contrast, natural libraries can be prepared relatively quickly and screened for bioactivity using pure compounds or extracts. The primary role of phytochemicals like acacetin is to inhibit the proliferation of plant pathogens including viruses, fungi and bacteria. This increases the possibility of bioactivity toward structurally conserved cell signaling intermediates, in comparison with randomly generated synthetic structures.

In summary, we have shown that acacetin inhibits EGF-induced anchorage-dependent and -independent melanoma cell growth. These results are reflected *in vivo* through reductions in tumor growth using a mouse xenograft model. We propose that this inhibition is mediated primarily through the attenuation of the PI3-K/Akt/$p70^{S6K}$ signaling pathway by direct physical inhibition of PI3-K in an ATP-competitive manner. Taken together, these results suggest that acacetin is a potent inhibitor of PI3-K and has potential for development as an antineoplastic agent to suppress the growth of melanoma cells.

Funding

Hormel Foundation; Leap Research Program (No. 2010-0029233), Basic Science Research Program (NRF-2011-357-F00044) and Global Frontier Project grant (NRF-M1AXA002-2012M3A6A4054949) through the National Research Foundation of Korea funded by the Ministry of Education, Science and Technology, Republic of Korea; Korea Food Research Institute; National Institutes of Health grants (CA120388, R37CA081064, CA1666011, CA172457).

Conflict of Interest Statement: None declared.

References

1. Stern,R.S. (2010) Prevalence of a history of skin cancer in 2007: results of an incidence-based model. *Arch. Dermatol.*, **146**, 279–282.
2. Soengas,M.S. *et al.* (2003) Apoptosis and melanoma chemoresistance. *Oncogene*, **22**, 3138–3151.
3. Tsao,H. *et al.* (2012) Melanoma: from mutations to medicine. *Genes Dev.*, **26**, 1131–1155.
4. Klein,S. *et al.* (2009) Targeting the EGFR and the PKB pathway in cancer. *Curr. Opin. Cell Biol.*, **21**, 185–193.
5. Paolini,F. *et al.* (2011) Human Papillomaviruses, p16INK4a and Akt expression in basal cell carcinoma. *J. Exp. Clin. Cancer Res.*, **30**, 108.
6. Tsai,W.B. *et al.* (2012) Activation of Ras/PI3K/ERK pathway induces c-Myc stabilization to upregulate argininosuccinate synthetase, leading to arginine deiminase resistance in melanoma cells. *Cancer Res.*, **72**, 2622–2633.
7. Jung,S.K. *et al.* (2010) Myricetin inhibits UVB-induced angiogenesis by regulating PI-3 kinase *in vivo*. *Carcinogenesis*, **31**, 911–917.
8. Pan,M.H. *et al.* (2006) Acacetin suppressed LPS-induced up-expression of iNOS and COX-2 in murine macrophages and TPA-induced tumor promotion in mice. *Biochem. Pharmacol.*, **72**, 1293–1303.
9. Shen,K.H. *et al.* (2010) Acacetin, a flavonoid, inhibits the invasion and migration of human prostate cancer DU145 cells via inactivation of the p38 MAPK signaling pathway. *Mol. Cell. Biochem.*, **333**, 279–291.
10. Chien,S.T. *et al.* (2011) Acacetin inhibits the invasion and migration of human non-small cell lung cancer A549 cells by suppressing the p38α MAPK signaling pathway. *Mol. Cell. Biochem.*, **350**, 135–148.
11. Jung,S.K. *et al.* (2008) Myricetin suppresses UVB-induced skin cancer by targeting Fyn. *Cancer Res.*, **68**, 6021–6029.
12. Kiefer,F. *et al.* (2009) The SWISS-MODEL Repository and associated resources. *Nucleic Acids Res.*, **37**(Database issue), D387–D392.
13. Friesner,R.A. *et al.* (2004) Glide: a new approach for rapid, accurate docking and scoring. 1. Method and assessment of docking accuracy. *J. Med. Chem.*, **47**, 1739–1749.
14. Sherman,W. *et al.* (2006) Novel procedure for modeling ligand/receptor induced fit effects. *J. Med. Chem.*, **49**, 534–553.
15. Dong,Z. *et al.* (2002) Harvesting cells under anchorage-independent cell transformation conditions for biochemical analyses. *Sci. STKE*, **2002**, pl7.
16. Kang,N.J. *et al.* (2007) Equol, a metabolite of the soybean isoflavone daidzein, inhibits neoplastic cell transformation by targeting the MEK/ERK/p90RSK/activator protein-1 pathway. *J. Biol. Chem.*, **282**, 32856–32866.
17. Gong,C. *et al.* (2012) LY294002 induces G0/G1 cell cycle arrest and apoptosis of cancer stem-like cells from human osteosarcoma via down-regulation of PI3K activity. *Asian Pac. J. Cancer Prev.*, **13**, 3103–3107.
18. Bode,A.M. *et al.* (2003) Mitogen-activated protein kinase activation in UV-induced signal transduction. *Sci. STKE*, **2003**, RE2.
19. Bode,A.M. *et al.* (2009) Cancer prevention research - then and now. *Nat. Rev. Cancer*, **9**, 508–516.
20. Surh,Y.J. (2003) Cancer chemoprevention with dietary phytochemicals. *Nat. Rev. Cancer*, **3**, 768–780.
21. Noble,M.E. *et al.* (2004) Protein kinase inhibitors: insights into drug design from structure. *Science*, **303**, 1800–1805.
22. Lacouture,M.E. (2006) Mechanisms of cutaneous toxicities to EGFR inhibitors. *Nat. Rev. Cancer*, **6**, 803–812.
23. Bode,A.M. *et al.* (2000) Signal transduction pathways: targets for chemoprevention of skin cancer. *Lancet Oncol.*, **1**, 181–188.
24. Ichimatsu,D. *et al.* (2007) Structure-activity relationship of flavonoids for inhibition of epidermal growth factor-induced transformation of JB6 Cl 41 cells. *Mol. Carcinog.*, **46**, 436–445.
25. He,Z. *et al.* (2008) Fyn is a novel target of (-)-epigallocatechin gallate in the inhibition of JB6 Cl41 cell transformation. *Mol. Carcinog.*, **47**, 172–183.
26. Nikolaou,V.A. *et al.* (2012) Melanoma: new insights and new therapies. *J. Invest. Dermatol.*, **132**(3 Pt 2), 854–863.
27. Villanueva,J. *et al.* (2010) Acquired resistance to BRAF inhibitors mediated by a RAF kinase switch in melanoma can be overcome by cotargeting MEK and IGF-1R/PI3K. *Cancer Cell*, **18**, 683–695.
28. Eggermont,A.M. *et al.* (2012) Melanoma in 2011: a new paradigm tumor for drug development. *Nat. Rev. Clin. Oncol.*, **9**, 74–76.
29. Davies,M.A. (2012) The role of the PI3K-AKT pathway in melanoma. *Cancer J.*, **18**, 142–147.
30. Haluska,F. *et al.* (2007) The RTK/RAS/BRAF/PI3K pathways in melanoma: biology, small molecule inhibitors, and potential applications. *Semin. Oncol.*, **34**, 546–554.
31. Sinnberg,T. *et al.* (2009) Inhibition of PI3K-AKT-mTOR signaling sensitizes melanoma cells to cisplatin and temozolomide. *J. Invest. Dermatol.*, **129**, 1500–1515.
32. Lee,K.M. *et al.* (2010) 5-deoxykaempferol plays a potential therapeutic role by targeting multiple signaling pathways in skin cancer. *Cancer Prev. Res. (Phila).*, **3**, 454–465.
33. Kim,H.Y. *et al.* (2012) Raf and PI3K are the molecular targets for the antimetastatic effect of luteolin. *Phytother. Res.* doi:10.1002/ptr.4888
34. Walker,E.H. *et al.* (2000) Structural determinants of phosphoinositide 3-kinase inhibition by wortmannin, LY294002, quercetin, myricetin, and staurosporine. *Mol. Cell*, **6**, 909–919.
35. Vanhaesebroeck,B. *et al.* (2005) Signalling by PI3K isoforms: insights from gene-targeted mice. *Trends Biochem. Sci.*, **30**, 194–204.

Received February 28, 2013; revised July 22, 2013; accepted July 30, 2013